Electro-polymerized polyaniline modified conductive bacterial cellulose anode for supercapacitive microbial fuel cells and studying the role of anodic biofilm in the capacitive behavior

# Electro-polymerized Polyaniline Modified Conductive Bacterial Cellulose Anode for Supercapacitive Microbial Fuel Cells and Studying the Role of Anodic Biofilm on the Capacitive Behavior

Mehrdad Mashkour[1,3], Mostafa Rahimnejad[*1], Mahdi Mashkour[2], and Francesca Soavi[3]

[1] Biofuel and Renewable Energy Research Center, Babol Noshirvani University of Technology, Babol, Iran

[2] Laboratory of Sustainable Nanomaterials, Faculty of Wood and Paper Engineering, Gorgan University of Agricultural Sciences and Natural Resources, Gorgan, Iran

[3] Department of Chemistry "Giacomo Ciamician", Alma Mater Studiorum - Università di Bologna, 40126, Bologna, Italy

* Corresponding author Email address: Rahimnejad_mostafa@yahoo.com, Rahimnejad@nit.ac.ir

Tel: +98 (0) 11 32334204; Fax: +98 (0) 11 32334204

**Abstract**

Polyaniline (PANI) modified conductive bacterial cellulose (BC) - carbon nanotubes (CNT) membranes are proposed as cost-effective alternatives for microbial fuel cell (MFC) anodes. The capacitive behavior of BC-CNT-PANI in a supercapacitive microbial fuel cell (SCMFC) and its effect on power performance was studied. BC was coated by carbon nanotubes (CNT) by vacuum filtering to form a conductive electrode (BC-CNT). Then the conductive side was coated by PANI through fast and easy electro-polymerization

(BC-CNT-PANI). Both electrodes were studied by impedance analysis before and after biofilm formation on their surface. Unlike BC-CNT, BC-CNT-PANI capacitance increased after biofilm formation achieving a capacitance that was double than that of BC-CNT with a charge transfer resistance about three times lower. Supercapacitive MFC was assembled and tested with BC-CNT, BC-CNT-PANI, and the double-anode BC-CNT& BC-CNT-PANI. The power performance of the SCMFC was limited by the anodes. The power performance was significantly improved by 20% by the use of the PANI-based anodes compare to the cell with BC-CNT.

*Keywords*: Bacterial cellulose; capacitive behavior; polyaniline; impedance; supercapacitive microbial fuel cell; anodic biofilm

## 1. Introduction

Microbial fuel cell (MFC) as a developing technology for producing bioelectricity from organic compounds of waste materials has cough the eye of scientists in recent two decades [1]. In MFCs, microorganisms are the active biocatalysts decomposing organic matters. They form an electro-active biofilm on the anode surface. Protons, oxidized molecules and electrons are the main products of the biofilm redox reaction. Protons and electrons are transferred to the cathode, respectively, by the solution and external circuit to take part in an oxygen reduction reaction at the cathode surface [2]. In this cycle, the active biofilm is of great importance. Effective parameters on the quality and activity of anodic biofilms are the source of microorganisms [3], the chemical composition of feeding molecules [4], and the electrode material [5]. Choosing a suitable electrode can improve the MFC's performance and decrease costs noticeably [6]. An excellent MFC anode should feature good conductivity, low cost, flexibility, the high surface area for microbial colonization, biocompatibility, hydrophilicity, and high capacitance [7-9]. The latter feature has indeed been exploited to design supercapacitive MFCs (SCMFC) with boosted power performance [10, 11]. Conventional anode materials like graphite, carbon cloth, and paper inherited by more mature fuel cell

technologies, cannot provide all the mentioned required properties for a bio-anode in MFC [12]. Hence, new anodes electrodes that address MFCs' requirements are needed. The main challenge is to design a low-cost fabrication process to make this technology capable of competing with other renewable energy harvesters.

Bacterial cellulose (BC) is a low-cost biopolymer with high flexibility and hydrophilic porous structure. These unique features have encouraged the researchers to exploit BC for electrode fabrication for fuel cells, batteries, and supercapacitors [13-16]. Easy binder-less coating of BC has been demonstrated by many nano-scale carbons like CNTs and graphene and also conductive polymers like polyaniline (PANI) and polypyrrole [17]. These approaches make it possible to avoid expensive binders such as polytetrafluoroethylene (PTFE) and Nafion, which usually make up 10-20 percent of the coating mass [18, 19], and make BC an excellent green substrate for electrode manufacturing. However, it should be noted that it is sensitive to very high acidic or basic solutions, at high temperature [20].

Vacuum filtration, drop-casting, soaking, and in situ synthesis are the popular methods exploited for coating cellulosic materials [21, 22]. A flexible conductive paper based on BC with CNT and Gum Arabic was fabricated by a drop-casting method with a low sheet resistance of 1 Ω.cm [23]. BC-CNT composites were also prepared by the vacuum filter method for enzyme immobilization and were utilized as both anode and cathode in enzymatic fuel cells [18]. Carbon coating on BC by vacuum filtering results in a homogeneous coating with a stable and robust connection between nanocarbon particles and BC. Chemical polymerization of conductive polymers on BC was also pursued. By this method, a cheap BC-PANI anode was fabricated for an H-type double chamber MFC. The BC-PANI anode was demonstrated to improve MFC power density for cells featuring a graphite anode [24].

PANI is a low-cost conductive polymer. Its conductivity is strongly pH-dependent. In acidic media, it is a good conductive material, while in neutral pH, its conductivity is low [25, 26]. However, due to the high redox and catalytic activity of PANI and its biocompatibility, in many MFC literature, it has been considered a superior anode modifier [27-30]. Moreover, PANI possesses pseudocapacitance behavior

driven by bulk faradic reactions and proton exchange [31]. The pseudocapacitance of PANI is much higher than the electrical double layer capacitance of carbon electrodes that, in turn, is given by electrostatic surface processes. However, the cycling stability of PANI is known not to be competitive with that of carbon electrodes [32]. For the use of PANI in MFC anodes, it is also necessary to consider the biofilm role. To the best of our knowledge, there are no thorough studies for the pseudocapacitive response of PANI modified bioanodes.

In this study, BC was coated by vacuum filtering of CNTs and then decorated with PANI by electro-polymerization. The BC-CNT-PANI was investigated as a superpcapacitive bioanode of SCMFCs for the first time. The morphology of the coatings and the colonized bacteria were studied. The main novelty of this work is investigating the effect of anodic biofilm on the capacitive response of CNTs and PANI modified CNTs. The study was carried out by cyclic voltammetry and impedance spectroscopy analysis. Additionally, the effect of the bio-anodes' capacitance on the MFC's performance was measured by galvanostatic discharges. Moreover, the PANI modified electrode was short-circuited to BC-CNT to give a double anode that was coupled with the air-breathing cathode to improve the SCMFC's performance.

## 2. Materials and methods

### *2.1. Fabrication of BC-CNT and PANI coating*

At first, 10 mg of CNT (multi-walled, Neutrino, Iran) were mixed with sodium dodecyl sulfate (Merck, Germany) in 25 ml of Milli-Q water under 15 min by ultrasound to form a homogeneous suspension. Afterward, a sheet of wet BC (Nano Novin Polymer, Iran) with a thickness of 2 mm was placed on the glass filter of an Erlen Bochner flask. CNT coating on BC was carried out by vacuum filtering. Then it was left at ambient temperature up to complete drying. The BC-CNT membrane was fixed at the bottom of a handmade electrochemical three electrodes cell (with a capacity of 12 ml). The BC-CNT, spiral-shaped titanium mesh (with an extra surface), and silver wire r were placed respectively as working, counter, and

reference electrodes in the cell (Fig.1 A). Because of the hydrophilic nature of BC, a Mylar sheet was placed under the BC-CNT substrate to prevent the solution leaking from the cell. The CNT coated surface was exposed to the monomer solution (230 μl of aniline in 10 ml of 1M HCl). For electro-polymerization of aniline on BC-CNT, pulse galvanostatic technique (20 pulses and 50 s for each pulse) with a current density of 2 $mA/cm^2$ (per BC-CNT surface) was exploited and performed by a potentiostat Volta Lab. After electro-polymerization, a green layer of emeraldine was formed on BC-CNT. The film was washed several times with Milli-Q water to separate unreacted monomers and increase the pH of BC-CNT-PANI to neutral. Then it was dried under ambient temperature. PANI electro-polymerization on BC-CNT was characterized by FESEM.

*2.2. MFC and incubation*

A single chamber MFC fabricated by Plexiglas, with 250 ml working volume, was used in this study. It was incubated by 125 ml of anaerobic sludge of biogas plant (Biotec Sys Srl, Bologna, Italy) and 125 ml of phosphate buffer solution (PBS) with potassium acetate (Merck, Germany) as bacterial feed (2.5 g/l). The cathode and anode size was 2.5 cm × 2.5 cm. The MFC had two anodes consisting of BC-CNT and BC-CNT-PANI and two membrane-less air-breathing cathodes. Both the anodes were placed in equal distance from the cathodes and also from the reference electrode. The cathodes were fabricated by coating a layer of carbon mixture (activated carbon 70%, carbon black 10%, and PTFE 20%) on Stain-less mesh (SSM) as the current collector. The air-cathode was sandwiched between two silicone gasket frames to avoid leakage. Also, for the anode, both coated BC sheets were separately placed on an SSM current collector and then pressed well between two plastic meshes to have a good connection with SSM (Fig.1 B). After incubation, the MFC was left in open-circuit voltage (OCV) for overnight. Then the circuits were closed by 1 kΩ resistance for colonization. In closed-circuit mode, once the voltage reached under 100 mV, acetate was added. It took 21 days for colonization, and then the resistors were removed, and the system continued on OCV mode.

*2.3. Electrochemical analyses*

All electrochemical analyses were performed in the SCMFC with the anode, cathode, and Ag respectively as working, counter, and reference electrode by a potentiostat/galvanostat (Biologic, France). For EIS, the test was done in the frequency range of 100 kHz to 20 mHz at OCV. Cyclic voltammetry (CV) was carried out in the potential window -0.6V to 0.3 V vs. ref at 0.2 mV/s to study the electro-catalytic behavior of the anodes. CV analysis also provided the capacitive response of the materials that was calculated by the slope of the plot of the voltammetric charge (current integrated over time) vs. potential [33]. Linear sweep voltammetry (LSV) was carried out in two and three-electrode modes respectively to record the full cell and single electrode polarization with a scan rate of 0.2 mV/s from OCV to V=0. Also, MFC power density was calculated with LSV from Eq(1)[34]:

$$P = \frac{V_{Cell} \times I}{V_c} \quad (1)$$

where $V_{Cell}$ is the cell voltage, $V_C$ represents cell volume ($m^3$), and $I$ is the current (mA). Galvanostatic discharge (GLV) test was performed by different pulse time ($t_{Pulse}$= 0.1, 0.5, 1 and 2 s) and discharging current ($I_{Pulse}$). By GLV test power and capacitance of the cell was calculated from Eq(2) and Eq(3)[10]:

$$P_{pulse} = ( I_{pulse} * \int_0^t V dt )/t_{pulse} \quad (2)$$

$$C_{Cell} = I_{Pulse} \times \left(\frac{dV}{dt}\right)^{-1} \quad (3)$$

## 3. Results and discussion

*3.1. Characterization of PANI coating*

Figure 1C and 1D report the FESEM images of the CNT coated BC surface after vacuum filtration and of the electro-polymerized PANI on BC-CNT, respectively. The comparison of Fig. 1C and 1D indicates that after electro-polymerization, CNTs were homogeneously coated with PANI with few agglomerates and that a core-shell structure was achieved. PANI was then expected to cross-link the CNTs to each other and to

BC substrate to form a more stable coating compared to the coating of bare CNTs on BC without PANI. It is noteworthy that such core-shell coating was achieved by a fast procedure ad that no chemical initiator like iron chloride was needed.

**Fig. 1.** (**A**) The three-electrode electro-polymerization cell, (**B**) Picture of the BC-based anode with SSM current collector sandwiched between two plastic meshes, and FESEM images of (**C**) CNT coated BC surface after vacuum filtration and (**D**) electro-polymerized PANI on BC-CNT.

*3.2. EIS and CV analyses*

In order to study the effect of microbial biofilm on the anodes' electrochemical response, EIS measurements were carried out in MFC before and after colonization (after 21 and 50 days). Figures 2A and 2B report the Nyquist plots of the BC-CNT and BC-CNT-PAN anodes, respectively. All the plots feature a high-frequency depressed semicircle with a low-frequency tail. The diameter of the semicircle (that might also result from two overlapped semicircles) can be attributed to charge transfer resistance at the electrode/electrolyte interface ($R_{ct}$). The low-frequency tail can be related to diffusive processes and capacitive features of the electrodes.

Before colonization, $R_{ct}$ for BC-CNT was 14.52 Ω and for BC-CNT-PANI was 41.28Ω. As already mentioned, the conductivity of PANI in neutral pH is low, which is the reason for the higher $R_{ct}$ of PANI modified anode with respect to BC-CNT. However, after biofilm formation, the $R_{ct}$ of the electrodes demonstrated an opposite trend. Indeed, after 21 days, $R_{ct}$ of BC-CNT increased up to 48 Ω while $R_{ct}$ of BC-CNT-PANI decreased to 24Ω. A similar trend was also observed after 50 days. After this period BC-CNT and BC-CNT-PANI featured $R_{ct}$ of 72 Ω and 21 Ω, respectively. The reversed trend of $R_{ct}$ changes suggested a positive effect of PANI on biofilm charge transfer activity.

The low-frequency tail of the Nyquist plots was modeled with the constant phase element CPE. The CPE impedance is:

$$Z_{CPE} = \frac{1}{Q\ (j2\pi f)^n} \quad (4)$$

where $f$ is the frequency. When n approaches 1.0, the phase angle is close to $-90^{0,}$ and $Q$ is a capacitance. When n=0.5, the phase angle is $-45^0$, and $Q$ represents the admittance of the Warburg line that described diffusion-controlled processes. The n number for BC-CNT-PANI was 0.7 before biofilm formation and reached 0.79 and 0.81 after 21 days and 50 days, respectively.

For a better understanding of the biofilm effect on the performance of the electrodes, phase angle and capacitance versus frequency were studied and are reported in Fig. 2C, D, E, and F as Bode Plots. The decomposition of organic matter to electrons and protons by microorganisms in anodic biofilm is a slow reaction. Thus low frequencies region of EIS spectra is of great importance [35]. Hence, in Fig. 2E and F, the capacitance values were evaluated at frequencies lower than 10 Hz by using Eq(5) [36]:

$$C_R = \frac{-Z''(\omega)}{2\pi f|Z(\omega)|^2} \quad (5)$$

Fig. 2 C-E show that BC-CNT and BC-CNT-PANI electrodes exhibited different behaviors before and after colonization. Before colonization, BC-CNT compared to BC-CNT-PANI had higher capacitance, smaller deviation from an ideal capacitor. Indeed, BC-CNT's capacitance was 87 mF, and its phase angle was -52˚while for the BC-CNT-PANI, the values were 36 mF and -46˚, respectively. However, the capacitance and phase angle of BC-CNT after 21 days reached 34 mF and -36˚and after 50 days, further decreased to 24 mF and -30˚. On the other hand, BC-CNT-PANI after 21 days reached a capacitance of 49 mF at a phase angle of -55˚that further increased after 50 days to 50 mF at -60˚.

Therefore, not only the charge transfer resistance $R_{ct}$ but also the capacitive behavior and phase angle of PANI modified anode improved along with biofilm. The opposite trend was observed for BC-CNT. These results can be explained by taking into account that PANI is hydrophilic. Therefore, PANI coating may

enhance the transfer of nutrients to the exoelectrogens of the anodic biofilm. The result is the enhancement of the production of electrons, protons, and, thus, electrical charge. Moreover, unlike CNTs that have a toxicity effect on microorganisms [37, 38], PANI is biocompatible and actively contributes to the bioactivity of the anode surface.

**Fig. 2.** Nyquist plots (**A**, **B**) and Bode Plots in terms of phase angle vs. frequency (**C**&**D**) and capacitance vs. frequency (**E**&**F**) for BC-CNT (**A**, **C**, **E**) and BC-CNT-PANI (**B**, **D**, **F**) electrodes tested in MFC by a three-electrode setup, before and after colonization.

After biofilm formation (after 50 days), CV and EIS analyses were carried out for BC-CNT, BC-CNT-PANI, and the "double-anode" obtained by short-circuiting the two BC-CNT and BC-CNT-PANI (BC-CNT & BC-CNT-PANI) electrodes. Fig. 3 A reports the voltammetric tests at 0.2 mV/s and evidences the higher redox activity of the PANI modified electrode compared to BC-CNT. The CV reported in the inset of Fig. 3A shows that GC-PANI at pH=7 had higher voltammetric peaks in Ar compared to in oxygen saturated PBS. This observation was already reported in the literature and related to the fact that PANI is not electro-active to oxygen at neutral pH, and it cannot catalyze ORR [39]. This feature may protect the anodic biofilm by avoiding recombination of the produced electrons and protons, especially once oxygen penetration from air-cathode to anodic chamber is possible. The voltammetric capacitance of BC-CNT, BC-CNT-PANI, and BC-CNT & BC-CNT-PANI was 349 mF, 800 mF, and 1156 mF, respectively. The results also verified the EIS data at low frequencies. Fig. 3 B compares the Nyquist plots of BC-CNT, BC-CNT-PANI, and BC-CNT & BC-CNT-PANI. The Figure shows that $R_{ct}$ of the "dual-anode" BC-CNT & BC-CNT-PANI, quantified in 13.5Ω is lower than the value for each electrode individually (mentioned at above section). It also further confirms that BC-CNT-PANI has a lower $R_{ct}$ than BC-CNT.

**Fig. 3.** Cyclic voltammograms at 0.2 mV/s **(A)** and Nyquist plots **(B)** for BC-CNT, BC-CNT-PANI individually, and after short-circuiting in three-electrode mode after 50 days with active biofilm.

*3.3. Characterization of biofilm on the anodes*

FESEM images of the anodes after colonization demonstrated the successful biofilm formation on both BC-CNT and BC-CNT-PANI. As can be seen, the biofilm formed on PANI modified anode (Fig.4 B & D) is denser than that on BC-CNT (Fig.4 A&C). Especially, bacteria size on BC-CNT-PANI (Fig.4 C) compared to BC-CNT (Fig.4 A) is larger. This result further supports the biocompatibility effect of PANI on microbial growth highlighted by the electrochemical analyses.

**Fig. 4.** FE-SEM images of (**A**&**C**) BC-CNT surface and (**B**&**D**) BC-CNT-PANI surface after colonization and biofilm formation.

*3.4. Power density and polarization test*

Fig. 5 shows the results of the SCMFC polarization tests carried out with BC-CNT, BC-CNT-PANI, and BC-CNT & BC-CNT-PANI anodes and the same air-breathing cathode. The current and the power are normalized to the cell volume. Specifically, Fig. 5A reports the full SCMFC cell voltage and power density over current.

The maximum power density achieved with BC-CNT was 270 $mW/m^3$. By PANI coating, the value was improved up to 330 $mW/m^3$. With the dual-anode, the power density of SCMFC further increased to 435 $mW/m^3$. It was expected because short-circuiting BC-CNT and BC-CNT-PANI provides higher active biofilm surface, lower $R_{ct}$, and higher capacitance.

The slope of the middle part of the polarization curves is related to internal resistance, namely the equivalent series resistance (ESR) of the MFC. The SCMFC with PANI modified anode featured an ESR of 1.12 kΩ that was lower than the value for the cell with BC-CNT (1.33 kΩ). Moreover, short-circuiting the anodes provided the lowest ESR of 0.84 kΩ. This trend suggests that ESR is much affected by anode impedance that, as reported above, decreases in the order BC-CNT > BC-CNT-PANI> BC-CNT&BC-CNT-PANI.

To shed light on the contribution of each electrode to cell performance, Fig. 5B shows the cathode and anode potentials trends during the polarization test. The potential profile of the cathodes almost overlapped for the three cases while the anode profile was different. In all the cells, the anode was the electrode that

mainly affected the cell voltage losses during the polarization test, which demonstrates that the cathode was not limiting SCMFC performance. The slope of the anodes decreased in the order BC-CNT > BC-CNT-PANI> BC-CNT&BC-CNT-PANI, i.e., following the same trend observed for the full cells.

**Fig. 5.** Polarization curve and power density the full MFC cells (**A**) and single electrodes polarization curves (**B**) in the presence of different anodes (BC-CNT, BC-CNT-PANI, and dual-anode BC-CNT & BC-CNT-PANI) by LSV at 0.2 $mV.s^{-1}$ after biofilm formation (50 days).

*3.5. GLV tests*

As for the polarization test, GLV was carried out with MFC featuring three cases of anodes and the same air-breathing cathode. GLV discharge was carried out with four different pulse times consisting of 0.1, 0.5, 1, and 2 s with different pulse currents from 0.5 mA to 15 mA (with 0.5 mA steps). Fig. 6 reports the pulse power vs. current curves for different pulse times. Power and current are normalized to the cathode area.

The trend of maximum power produced by the SCMFC for each pulse time is similar to the result obtained by LSV. Furthermore, decreasing pulse time resulted in higher generated power. The highest value of the power of 3.5 mW was achieved with the BC-CNT&BC-CNT-PANI dual anode over 11 mA pulses of 0.1 s. At pulses of 4 mA and 2 s, the same cell can supply 1.5 mW that well compares with the requirement of consumer electronics. All the GLV tests indicated that higher current and power could be obtained by PANI modified anode compared to bare BC-CNT. It can be mainly attributed to the higher capacitance of the modified anode, which was verified by impedance and CV experiments and is further discussed in the following.

**Fig. 6.** Pulse power delivered by MFC with BC-CNT, BC-CNT-PANI, and BC-CNT &BC-CNT-PANI anodes under GLV discharge with pulses of (**A**) 0.1s, (**B**) 0.5s, (**C**) 1s and (**D**) 2s.

Fig. 7 A shows the changes in cell voltage under 1 s pulses carried out at 3 mA of SCMFCs featuring different anodes. At the beginning of the pulse, the cell voltage sharply decreases. This voltage change ($\Delta V_{ohmic}$) is ohmic and is directly related to the cell ESR. After the initial drop, the voltage linearly decreases

over time following an "apparent capacitive" behavior ($\Delta V_{capacitance}$). Given that the test is galvanostatic, the slope of voltage vs. time plot is related to the reciprocal of the SCMFC capacitance (see Eq. 3)[11].

Similar $\Delta V_{ohmic}$ of 53 mV, 57 mV, and 46 mV were recorded for BC-CNT, BC-CNT-PANI, and BC-CNT&BC-CNT-PANI anodes, respectively. On the contrary, $\Delta V_{capacitance}$ significantly changed with the type of anode over 1 s pulses. The highest value of 217 mV was featured by the SCMFC with BC-CNT. With BC-CNT-PANI $\Delta V_{capacitance}$ was 150 mV, and with BC-CNT&BC-CNT-PANI, the value was 104 mV. According to Eq(3), the smallest slope of the capacitive voltage drop corresponds to the highest capacitance of the system. Therefore, the $\Delta V_{capacitance}$ values further indicate that the modification of BC-CNT by PANI improved the capacitance of the anode.

The capacitive voltage decrease ($\Delta V_{capacitance}/t_{pulse}$) was also evaluated for different pulse times at 3mA, and the reverse of the values, $(\Delta V_{capacitance}/t_{pulse})^{-1}$ are reported in Fig. 7B. Figure evidences that increasing pulse time resulted in smaller slopes for all the SCMFCs. Additionally, at each pulse time, the slope decreased in the order BC-CNT> BC-CNT-PANI>BC-CNT&BC-CNT-PANI. The corresponding SCMFC capacitive responses are reported in Fig.7 C and the increase in the order BC-CNT< BC-CNT-PANI<BC-CNT&BC-CNT-PANI. The time dependence of the capacitance can be explained by taking into account that in supercapacitive MFCs, two types of processes take place simultaneously: capacitive (or pseudocapacitance for PANI-based systems) discharge and Faradic discharge. The former process relates to the fast setup of electrical double-layers at the elected/electrolyte interfaces. The latter corresponds to the slow MFC redox processes, namely oxidation of organics at the bioanode and oxygen reduction at the air-breathing cathode. In the shorter times, the capacitive feature of the MFC mainly drives the MFC voltage profile. Instead, at the longer times, the faradaic processes become important and actively contribute to sustain the cell voltage and mitigate its decrease. This time-dependent mixed behavior has already been discussed and termed as "apparent capacitance" of MFCs [40].

The effect of capacitance on power generation in the SCMFC is highlighted in Fig.7 D. The Figure reports the generated power vs. capacitance calculated respectively by Eq(2) and Eq(3). GLV curves with a pulse

time of 2 s and different discharging current were analyzed. As a remarkable result, higher capacitance provided higher power output by the SCMFC. Indeed, PANI modified electrodes by their positive effect on biofilm activity and capacitive feature of the bio-anode, demonstrated by CV and EIS analysis, provided the best power performance.

**Fig. 7.** GLV discharges at 3 mA: Cell voltage profile under of 1s pulses with the indication of the ohmic drop and capacitive voltage decrease during the pulse (**A**), capacitive voltage drop vs. different pulse time (**B**), cell capacitance vs. different pulse time (**C**) and power generation versus cell capacitance by different discharging currents and pulse time of 2s (**D**) for the SCMFCs with BC-CNT, BC-CNT-PANI, and BC-CNT&BC-CNT-PANI anodes.

## 4. Conclusions

Here, we presented a low-cost pseudocapacitive bio-anode based on BC, CNTs, and PANI as flexible hydrogel anode for SCMFCs with the air-breathing cathode. CNTs were coated on the thin BC membrane by vacuum filtering with no binders. Afterward, PANI was synthesized on the electrode by fast and easy pulse galvanostatic technique. CVs demonstrated the higher redox activity of BC-CNT-PANI compared to BC-CNT. EIS results showed that the capacitance of BC-CNT decreased after colonization, while that of BC-CNT-PANI increased. Also, $R_{ct}$ of BC-CNT and BC-CNT-PANI increased and decreased respectively after colonization. The higher capacitance of the PANI modified bio-anode was also confirmed by GLV discharges. The slope of polarization curves for single electrodes showed that the anodes were limiting factor for power generation in the SCMFC. The effect of biofilm formation on PANI and CNT capacitance and its effect on power generation in SCMFC was studied here for the first time. Moreover, a 'dual anode'' obtained by short-circuiting BC-CNT-PANI to BC-CNT, which increased active anodic surface, exhibited the highest capacitance and provided an SCMFC with the highest power.

## Acknowledgments

MM and FS would like to thank Carlo Santoro, Catia Arbizzani and Federico Poli who helped them in the experiments. This work was supported by Iran National Science Foundation (INSF), grant number: INSF-95819857, Babol Noshirvani University of Technology (grant number: BNUT/5150010/1394) and Italy-South Africa joint Research Program 2018-2020 granted by Italian Ministers of Foreign Affairs and of the Environment. Also, MM and MR thank Biofuel & Renewable Energy Research Center at BNUT and Laboratory of Electrochemistry of Materials for Energetics (UNIBO-Italy) for providing facilities and test devices. Finally, MM and MR would like to thank Danesh Gostar Hamgam ba Sanat spin-off (Babol, Iran) for facilities and supports.

**References**

[1]M. Rahimnejad, A.A. Ghoreyshi, G. Najafpour, T. Jafary, Appl. Energy, 88 (2011) 3999-4004.

[2]M. Mashkour, M. Rahimnejad, Biofuel Res. J, 2 (2015) 296-300.

[3]B.E. Logan, R. Rossi, P.E. Saikaly, Nat. Rev. Microbiol., 17 (2019) 307-319.

[4]R.C. Tice, Y. Kim, J. Power Sources, 271 (2014) 360-365.

[5]C. Santoro, C. Arbizzani, B. Erable, I. Ieropoulos, J. Power Sources, 356 (2017) 225-244.

[6]G. Palanisamy, H.-Y. Jung, T. Sadhasivam, M.D. Kurkuri, S.C. Kim, S.-H. Roh, J. Cleaner Prod., 221 (2019) 598-624.

[7]M. Rahimnejad, A. Adhami, S. Darvari, A. Zirepour, S.-E. Oh, AEJ, 54 (2015) 745-756.

[8]S. Li, C. Cheng, A. Thomas, Adv. Mater., 29 (2017) 1602547.

[9]H. Wang, E. Zhu, J. Yang, P. Zhou, D. Sun, W. Tang, J. Phys. Chem. C, 116 (2012) 13013-13019.

[10]F. Soavi, C. Santoro, Curr. Opin. Electrochem., 22 (2020) 1-8.

[11]L. Caizán-Juanarena, C. Borsje, T. Sleutels, D. Yntema, C. Santoro, I. Ieropoulos, F. Soavi, A. ter Heijne, Biotechnol. Adv., 39 (2020) 107456.

[12]Y. Hindatu, M. Annuar, A. Gumel, Renewable Sustainable Energy Rev., 73 (2017) 236-248.

[13]S. Deng, Y. Zhang, D. Xie, L. Yang, G. Wang, X. Zheng, J. Zhu, X. Wang, Y. Yu, G. Pan, Nano Energy.364-355 (2019) 58 ,

[14]F. Guan, S. Chen, N. Sheng, Y. Chen, J. Yao, Q. Pei, H. Wang, Chem. Eng. J., 360 (2019) 829-837.

[15]M. Mashkour, T. Kimura, M. Mashkour, F. Kimura, M. Tajvidi, ACS Appl. Mater. Interfaces, 11 (2018) 1538-1.545

[16]M. Mashkour, M. Rahimnejad, M. Mashkour, G. Bakeri, R. Luque, S.E. Oh, ChemElectroChem, 4 (2017) 648-654.

[17]C. Vilela, A.J. Silvestre, F.M. Figueiredo, C.S. Freire, J. Mater. Chem. A, 7 (2019) 20045-20074.

[18]X. Li, P. Lv, Y .Yao, Q. Feng, A. Mensah, D. Li, Q. Wei, Chem. Eng. J., 379 (2020) 122316.

[19]G. Bakeri, A. Ismail, T. Matsuura, M. Abdullah, B. Ng, M. Mashkour, Chem. Eng. Res. Des., 104 (2015) 367-375.

[20]M. Roman, W.T. Winter, Biomacromolecules, 5 (2004) 1671-1677.

[21]M. Mashkour, T. Kimura, F. Kimura, M. Mashkour, M. Tajvidi, RSC Adv., 4 (2014) 52542-52549.

[22]M. Mashkour, M. Tajvidi, F. Kimura, H. Yousefi, T. Kimura, ACS Appl. Mater. Interfaces, 6 (2014) 8165-817.2

[23]M. Mashkour, M. Sharifinia, H. Yousefi, E. Afra, Carbohydr. Polym., 202 (2018) 504-512.

[24]M. Mashkour, M. Rahimnejad, M. Mashkour, J. Power Sources, 325 (2016) 322-328.

[25]W.W. Focke, G.E. Wnek, Y. Wei, J. Phys. Chem., 91 (1987) 5813-5818.

[26]A. Eftekhari, L. Li, Y. Yang, J. Power Sources, 347 (2017) 86-107.

[27]L. Huang, X. Li, Y. Ren, X. Wang, Int. J. Hydrogen Energy, 41 (2016) 11369-11379.

[28]H.-F. Cui, L. Du, P.-B. Guo, B. Zhu, J.H .Luong, J. Power Sources, 283 (2015) 46-53.

[29]J. Hou, Z. Liu, P. Zhang, J. Power Sources, 224 (2013) 139-144.

[30]Y. Qiao, C.M. Li, S.-J. Bao, Q.-L. Bao, J. Power Sources, 170 (2007) 79-84.

[31]C. Peng, S. Zhang, D. Jewell, G.Z. Chen, Prog. Nat. Sci., 18 (2008) 777-788.

[32]H. Wang, J. Lin, Z.X. Shen, J. Sci.: Adv. Mater. Devices, 1 (2016) 225-255.

[33]F. Soavi, L.G. Bettini, P. Piseri, P. Milani, C. Santoro, P. Atanassov, C. Arbizzani, J. Power Sources, 326 (2016) 717-725.

[34]M. Masoudi, M. Rahimnejad, M. Mashkour, Electrochim. Acta, 344 (2020) 136168.

[35]R.P. Ramasamy, V. Gadhamshetty, L.J. Nadeau, G.R. Johnson, Biotechnol. Bioeng., 104 (2009) 882-891.

[36]L. Nègre ,B. Daffos, P.-L. Taberna, P. Simon, J. Electrochem. Soc., 162 (2015) A5037-A5040.

[37]B. Zhu, X. Xia, N. Xia, S. Zhang, X. Guo, Environ. Sci. Technol., 48 (2014) 4086-4095.

[38]L.A. Luongo, X.J. Zhang, J. Hazard. Mater., 178 (2010) 356-362.

[39]C. Cui, J.Y. Lee, J. Electroanal. Chem., 367 (1994) 205-212.

[40]F. Poli, J. Seri, C. Santoro, F. Soavi, ChemElectroChem, 7 (2020) 893-903.

**Figure captions**

**Fig. 1.** (**A**) The three-electrode electro-polymerization cell, (**B**) Picture of the BC-based anode with SSM current collector sandwiched between two plastic meshes, and FESEM images of (**C**) CNT coated BC surface after vacuum filtration and (**D**) electro-polymerized PANI on BC-CNT.

**Fig. 2.** Nyquist plots (**A**, **B**) and Bode Plots in terms of phase angle vs. frequency (**C**&**D**) and capacitance vs. frequency (**E**&**F**) for BC-CNT (**A**, **C**, **E**) and BC-CNT-PANI (**B**, **D**, **F**) electrodes tested in MFC by a three-electrode setup, before and after colonization.

**Fig. 3.** Cyclic voltammograms at 0.2 mV/s **(A)** and Nyquist plots **(B)** for BC-CNT, BC-CNT-PANI individually, and after short-circuiting in three-electrode mode after 50 days with active biofilm.

**Fig. 4.** FE-SEM images of (**A**&**C**) BC-CNT surface and (**B**&**D**) BC-CNT-PANI surface after colonization and biofilm formation.

**Fig. 5.** Polarization curve and power density the full MFC cells (**A**) and single electrodes polarization curves (**B**) in the presence of different anodes (BC-CNT, BC-CNT-PANI, and dual-anode BC-CNT & BC-CNT-PANI) by LSV at 0.2 $mV.s^{-1}$ after biofilm formation (50 days).

**Fig. 6.** Pulse power delivered by MFC with BC-CNT, BC-CNT-PANI, and BC-CNT &BC-CNT-PANI anodes under GLV discharge with pulses of (**A**) 0.1s, (**B**) 0.5s, (**C**) 1s and (**D**) 2s.

**Fig. 7.** GLV discharges at 3 mA: Cell voltage profile under of 1s pulses with the indication of the ohmic drop and capacitive voltage decrease during the pulse (**A**), capacitive voltage drop vs. different pulse time (**B**), cell capacitance vs. different pulse time (**C**) and power generation versus cell capacitance by different discharging currents and pulse time of 2s (**D**) for the SCMFCs with BC-CNT, BC-CNT-PANI, and BC-CNT&BC-CNT-PANI anodes.

**Figures:**

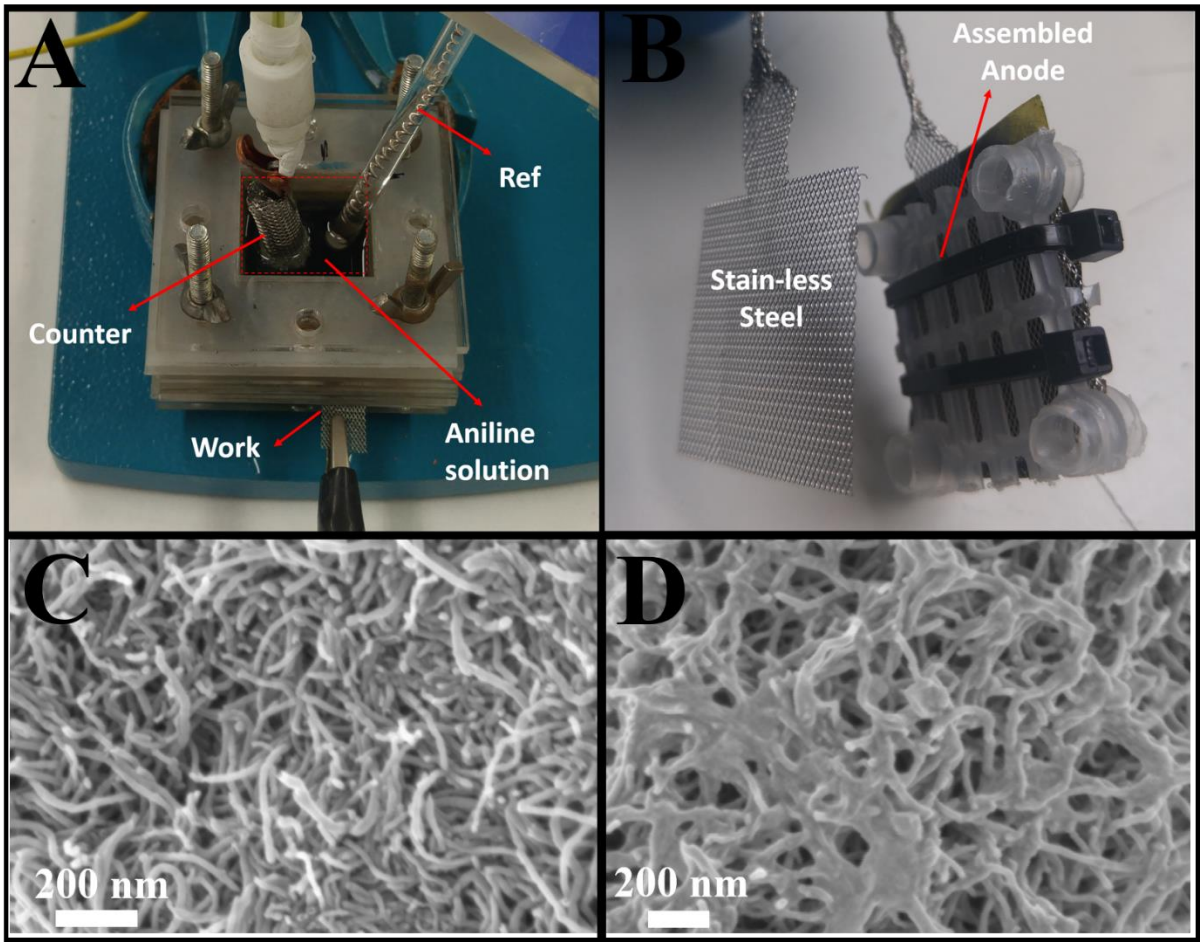


**Fig. 1**

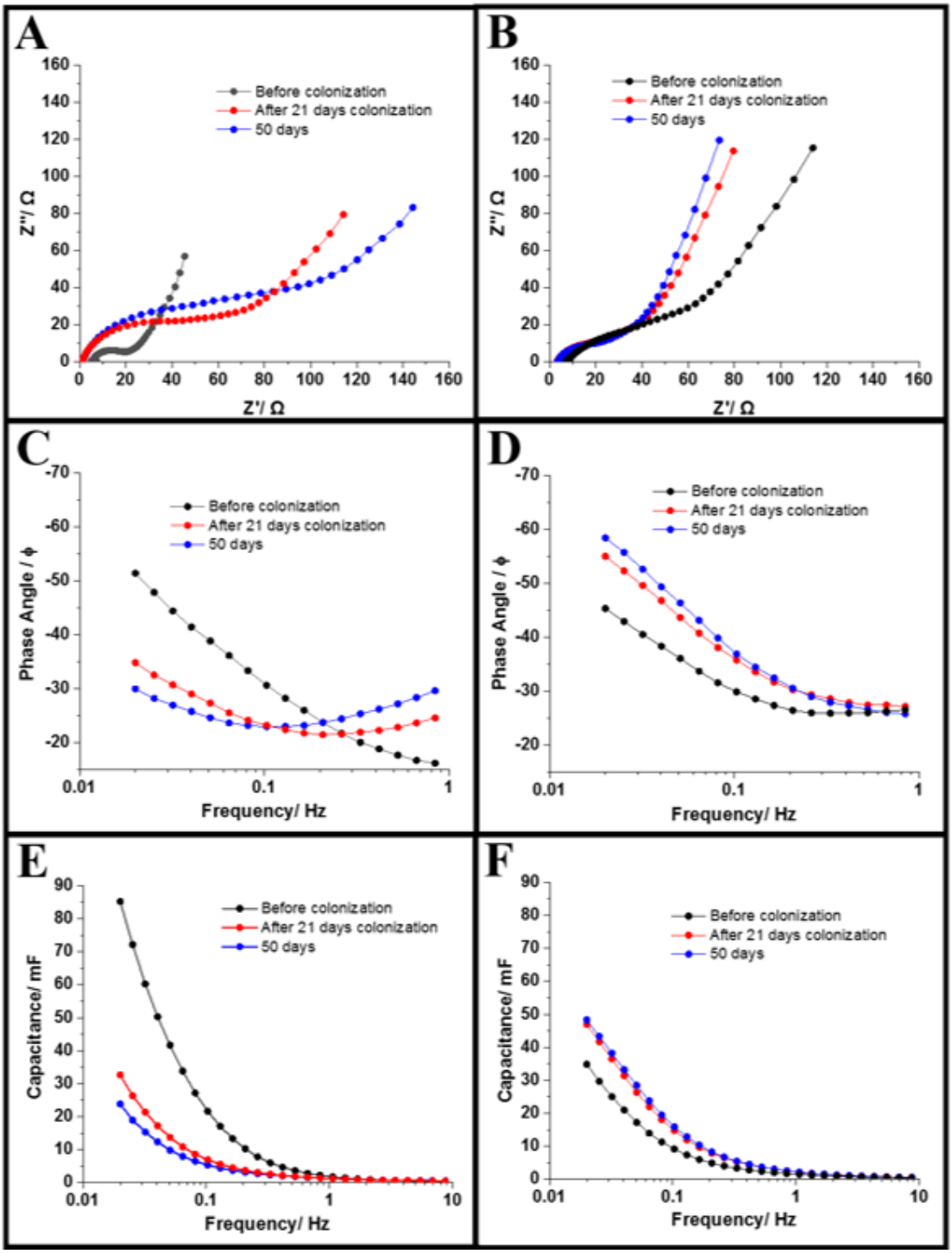
A
Before colonization
After 21 days colonization
50 days
Z''/ Ω
Z'/ Ω
B
Before colonization
After 21 days colonization
50 days
Z''/ Ω
Z'/ Ω
C
Before colonization
After 21 days colonization
50 days
Phase Angle / ϕ
Frequency/ Hz
D
Before colonization
After 21 days colonization
50 days
Phase Angle / ϕ
Frequency/ Hz
E
Before colonization
After 21 days colonization
50 days
Capacitance/ mF
Frequency/ Hz
F
Before colonization
After 21 days colonization
50 days
Capacitance/ mF
Frequency/ Hz

**Fig.2**

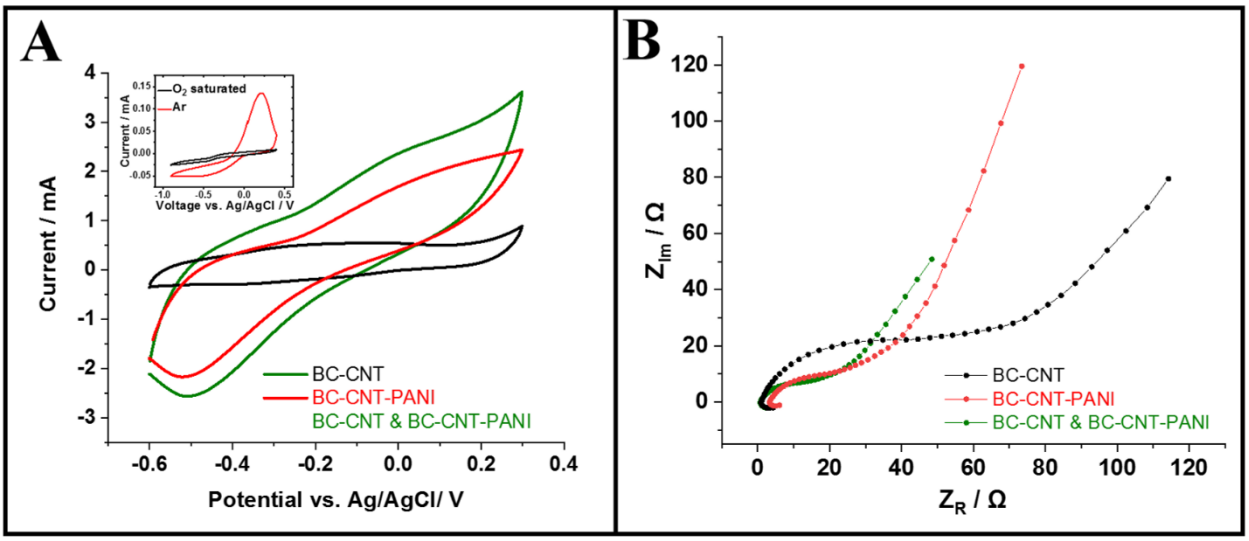
A
Current / mA
Potential vs. Ag/AgCl/ V
BC-CNT
BC-CNT-PANI
BC-CNT & BC-CNT-PANI
O2 saturated
Ar
Current / mA
Voltage vs. Ag/AgCl / V
B
Zim / Ω
ZR / Ω
BC-CNT
BC-CNT-PANI
BC-CNT & BC-CNT-PANI

**Fig.3**

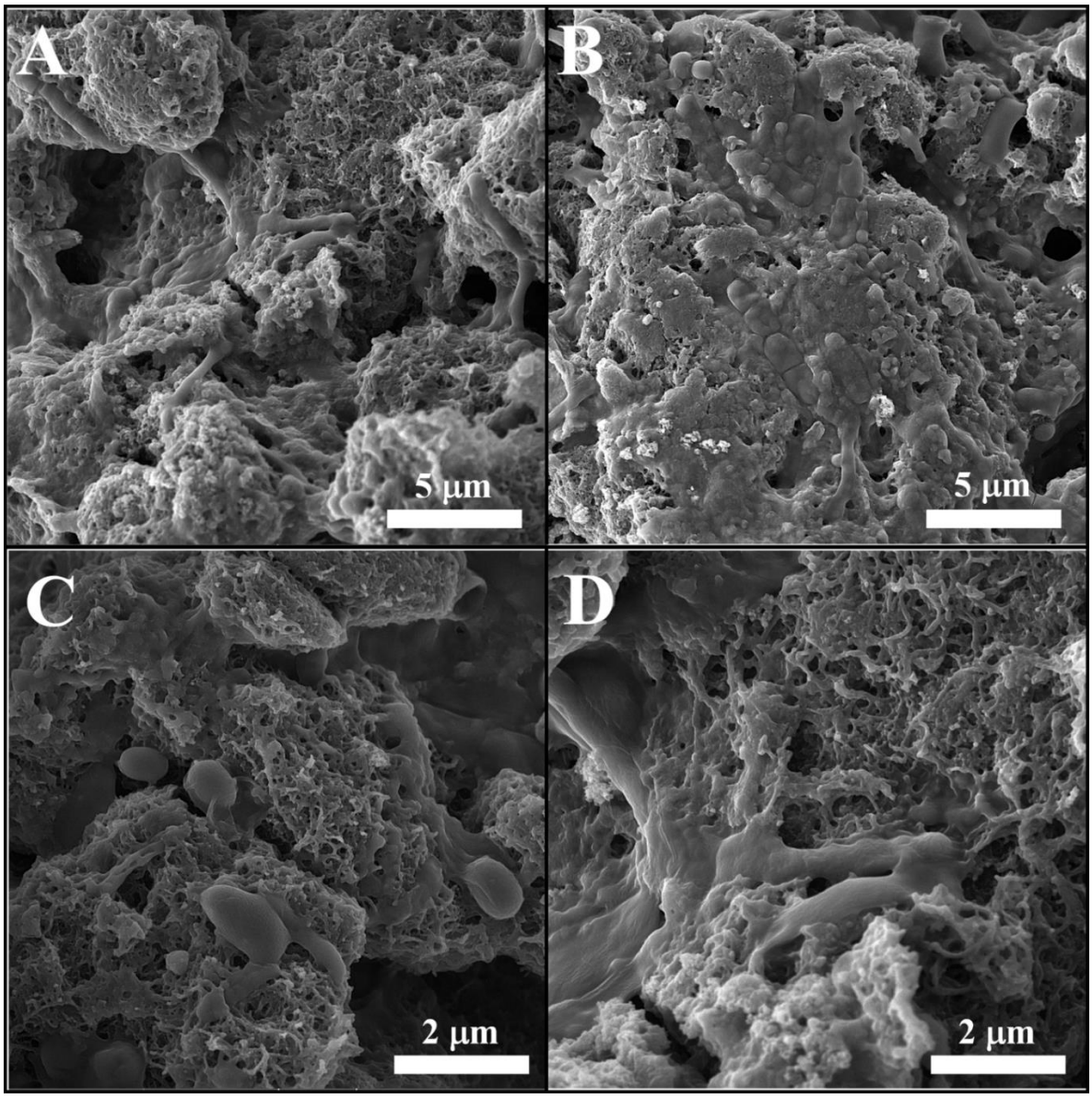


**Fig. 4**

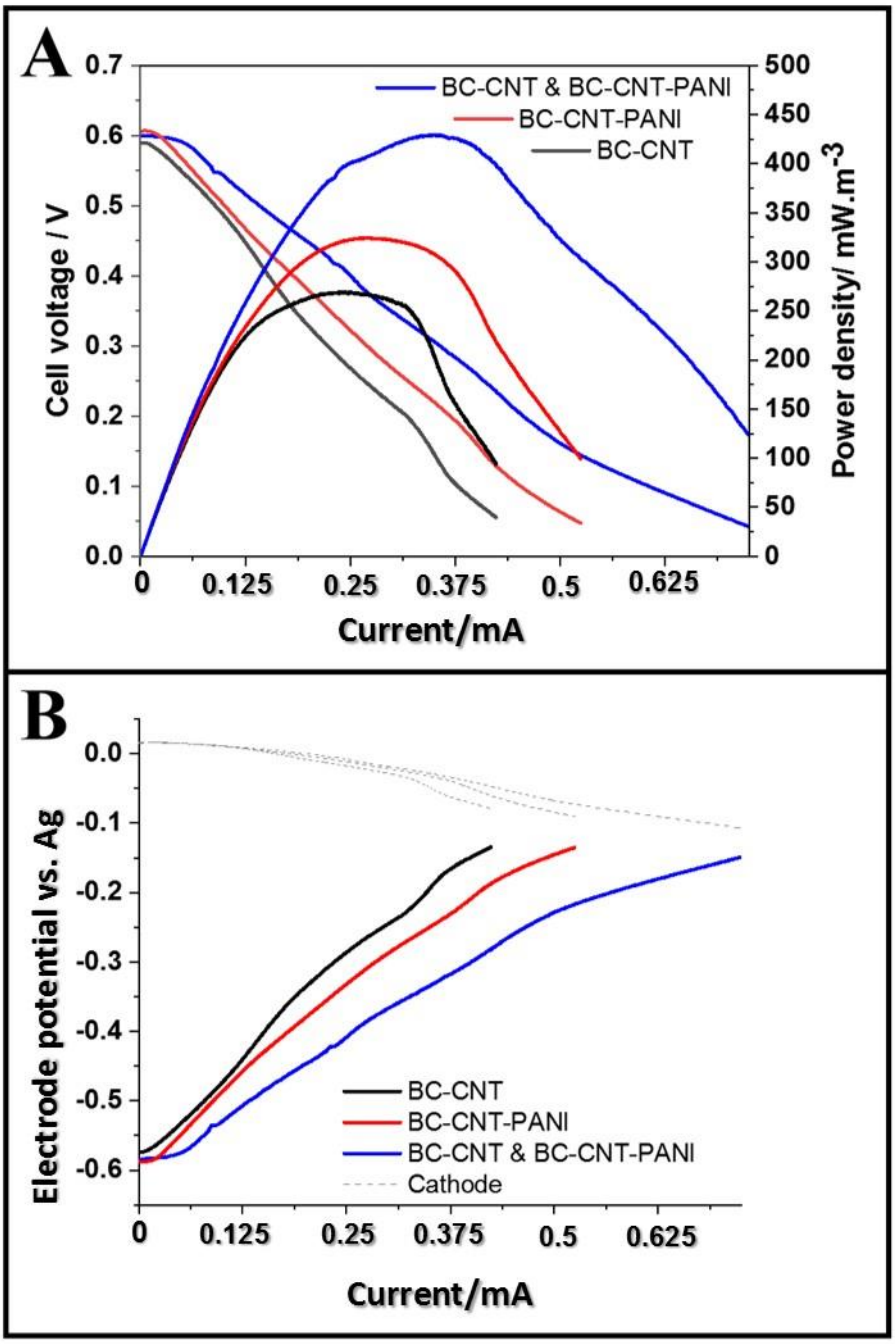
A
Cell voltage / V
Power density/ mW.m-3
Current/mA
BC-CNT & BC-CNT-PANI
BC-CNT-PANI
BC-CNT
B
Electrode potential vs. Ag
Current/mA
BC-CNT
BC-CNT-PANI
BC-CNT & BC-CNT-PANI
Cathode

**Fig.5**

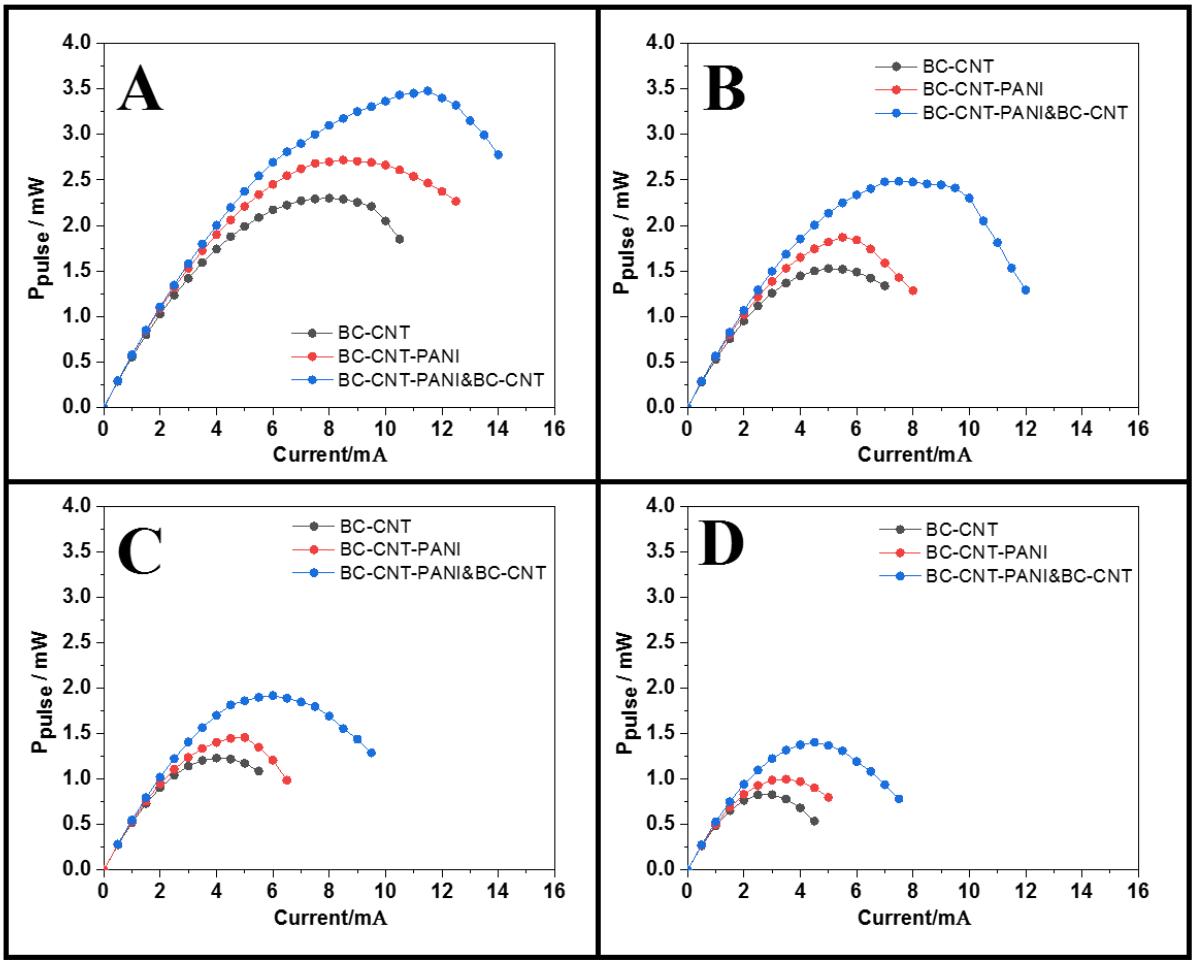
A
B
C
D
BC-CNT
BC-CNT-PANI
BC-CNT-PANI&BC-CNT
Ppulse / mW
Current/mA
0.0
0.5
1.0
1.5
2.0
2.5
3.0
3.5
4.0
0
2
4
6
8
10
12
14
16

**Fig.6**

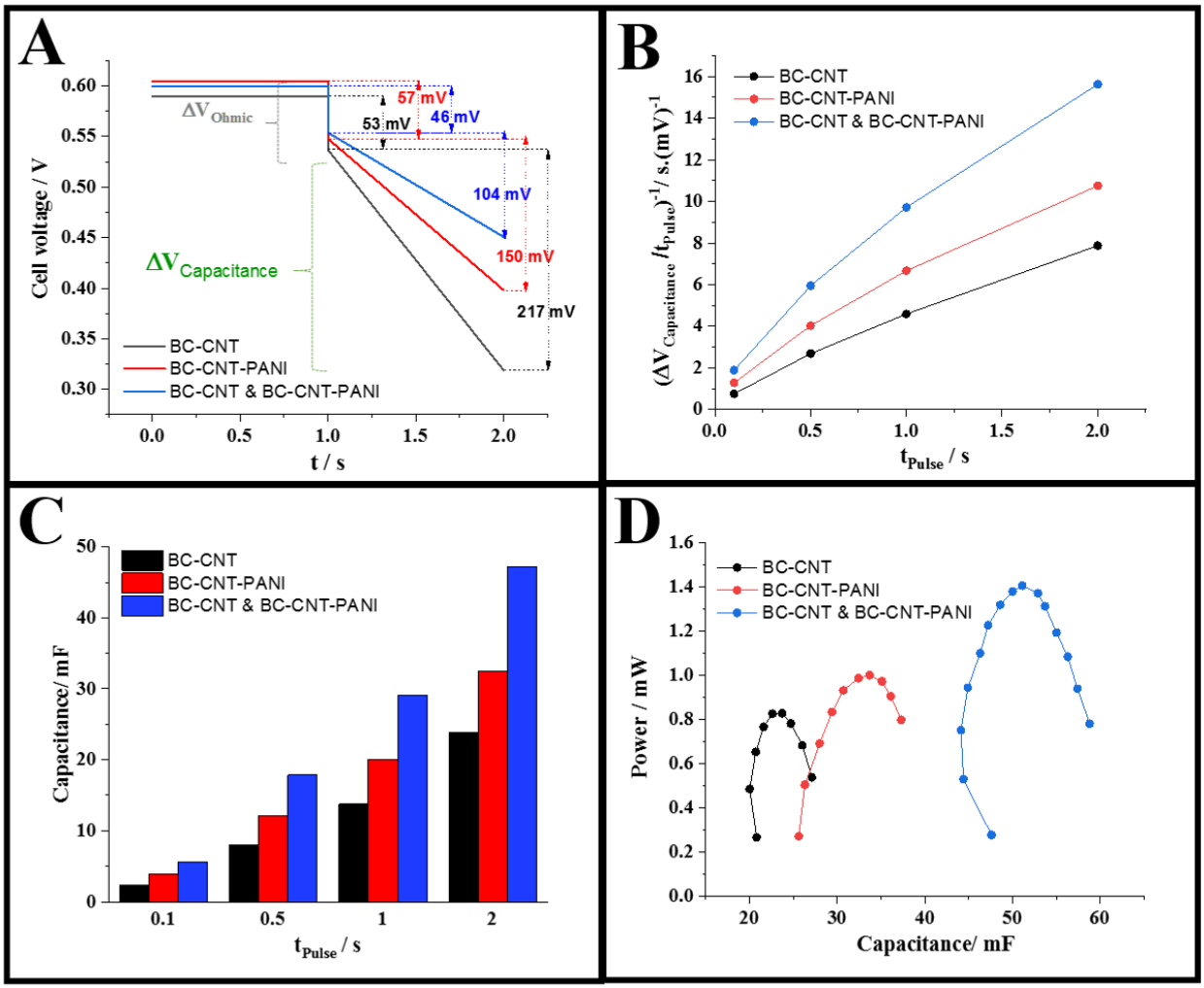
A
Cell voltage / V
t / s
ΔV Ohmic
ΔV Capacitance
57 mV
53 mV
46 mV
104 mV
150 mV
217 mV
BC-CNT
BC-CNT-PANI
BC-CNT & BC-CNT-PANI
B
(ΔV Capacitance /t Pulse)-1/ s.(mV)-1
t Pulse / s
BC-CNT
BC-CNT-PANI
BC-CNT & BC-CNT-PANI
C
Capacitance/ mF
t Pulse / s
BC-CNT
BC-CNT-PANI
BC-CNT & BC-CNT-PANI
D
Power / mW
Capacitance/ mF
BC-CNT
BC-CNT-PANI
BC-CNT & BC-CNT-PANI

**Fig.7**

**Declaration of interests**

☒ The authors declare that they have no known competing financial interests or personal relationships that could have appeared to influence the work reported in this paper.

☐The authors declare the following financial interests/personal relationships which may be considered as potential competing interests:

| |
|---|
| |